THE JOURNAL OF PHYSICAL CHEMISTRY B

ARTICLE

pubs.acs.org/JPCB

Analysis of Kinetic Isotope Effects in Enzymatic Carbon−Hydrogen Cleavage Reactions

Willem Siebrand* and Zorka Smedarchina

Steacie Institute for Molecular Sciences, National Research Council of Canada, Ottawa, K1A 0R6 Canada

ABSTRACT: The instanton approach, as previously applied to proton tunneling in molecular systems, is adapted to carbon−hydrogen bond cleavage catalyzed by enzymes. To compensate for the complexity of enzymatic reactions, simplifications are introduced based on the observation in numerous X-ray measurements that enzymes tend to form compact structures, which is assumed to have led toward optimization of specific parameters that govern the tunneling rate in the instanton formalism. On this basis, semiempirical equations are derived that link observed kinetic data directly to these parameters. These equations provide an analytical relation between the kinetic isotope effect and its temperature dependence for each hydrogen isotope, from which mechanistic and structural information can be extracted, including the nature of the hydrogen acceptor, the magnitude of the hydrogen transfer distance, the presence of endothermicity, and the contribution and frequency of skeletal vibrations that assist the tunneling. The method is used to analyze kinetic data reported for eight enzymatic CH-cleavage reactions; the enzymes or models thereof studied include methylmalonyl-coenzyme A mutase (coenzyme B_{12}), galactose oxidase, lipoxygenase-1 with six mutants, methylamine dehydrogenase, an oxoiron(IV)porphyrin radical cation, phenylalanine hydroxylase, a bis(μ-oxo)dicopper complex, and rice α-oxygenase.

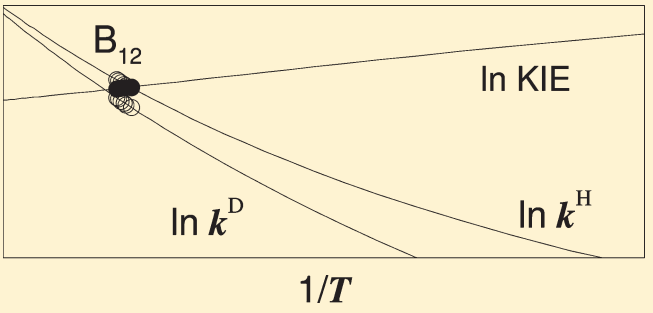

1. INTRODUCTION

Quantum effects show up in biology typically as large isotope effects on the rate of hydrogen or proton transfer reactions. Particularly striking are reductions by up to a factor of 10^2 occasionally observed for enzymatic carbon−hydrogen bond cleavage rates at room temperature. These observations point to tunneling through a potential-energy barrier as the rate-limiting step in the enzymatic reaction sequence. This complicates the analysis since even when the rate constant exhibits the exponential dependence on the inverse temperature normally observed for "classical" overbarrier processes the slope and intercept of the corresponding Arrhenius plot do not allow a classical interpretation: the slope does not indicate the barrier height, and the intercept does not indicate the rate for a vanishing barrier. On the other hand, the availability of CD-bond along with CH-bond data supplies additional information since the two tunneling reactions are electronically equivalent, which implies that they involve the same potential and differ only in the vibrational contributions. As a result, the kinetic isotope effect (KIE), i.e., the ratio of the H and D transfer rate constants, provides a widely used tool to study these reactions. Typically, the kinetic data available from direct measurements are rate constants for H and D transfer from a carbon donor to a known or unknown receptor in a narrow temperature interval near room temperature.

Although several methods are available to study tunneling reactions theoretically,[1] the complexity of enzymatic processes and the need to study them at different temperatures make it difficult to apply them directly to enzymes. The structure of the enzyme−substrate complex in which the tunneling takes place cannot be observed directly but must be inferred from the separate structures of the enzyme and the substrate if these are available at the resolution required, which is often not the case. Since the temperature dependence of tunneling reactions is typically governed by vibrations other than the high-frequency vibration of the tunneling coordinate, a detailed vibrational force field is necessary to calculate this temperature dependence from first principles. An authorative overview of the present situation has recently been published by Truhlar,[2] who is one of the principal contributors to this field. It seems fair to state that theory is not yet able to make reliable predictions of rate constants and their temperature- and isotope-dependence for enzymatic reactions whose rates are limited by tunneling. To bridge the gap between theory and experiment, we have been trying in a recent series of papers[3−5] to develop a semiempirical approach that can be used, on the one hand, by experimentalists to interpret their results in mechanistic terms and, on the other, by theorists to ascertain whether a reported experimental data set pertains indeed to a single transfer step in the enzymatic reaction sequence. The basic aim of the present paper is to apply this approach, after introducing several improvements to earlier

Received: March 8, 2011
Revised: May 5, 2011
Published: May 20, 2011

formulations, to the analysis of a representative series of enzymatic CH-bond cleavage reactions.

Carbon−hydrogen bonds have great strength and low polarity, two properties that hinder cleavage. Enzymes achieve cleavage in two ways: directly via hydrogen abstraction by a free radical and indirectly via electron abstraction from the CH bond leading to proton abstraction. Free radicals tend to be chemically agressive and may cause collateral damage; the direct process, which amounts to simple adiabatic transfer of a neutral hydrogen atom between two carbon centers, appears indeed to be relatively rare. The indirect process requires a redox system at the active site to abstract the electron from the CH bond and a hydroxyl group to abstract the emerging proton. The electron transfer implies that this reaction involves two electronic surfaces and is thus a nonadiabatic process.

In the case of adiabatic transfer between two carbon centers, it seems reasonable to assume that the barrier will be roughly symmetric. In the case of nonadiabatic involving transfer from a carbon to an oxygen center, the barrier is intrinsically asymmetric. However, given the strength of the CH bond, it is unlikely that the reaction will exhibit substantial exothermicity. If it is endothermic, this will lead to a contribution to the activation energy. To keep the analysis tractable, we will neglect the effect of any remaining exothermicity on the tunneling rate and include any endothermicity by means of a Boltzmann factor. Apart from this factor, we assume that the temperature dependence of the rate constants will be governed by vibrations that affect the height and width of the transfer barrier or that are displaced between the initial and final state.

To introduce empirical knowledge about vibrations directly or indirectly involved in the tunneling process, we previously[3,6] used Fermi's golden rule along with the Condon approximation to separate the matrix element driving the transfer into an electronic term which is temperature- and isotope-independent and a vibrational overlap factor. This is reasonable for adiabatic reactions taking place on a single surface[4] but becomes questionable for nonadiabatic reactions involving different electronic surfaces, in which the electronic coupling term is likely to be a function of vibrational coordinates. Although linear coupling was introduced and found to be of limited importance,[5] a more secure strategy would be to avoid the Condon approximation altogether. To this end, we introduce here a different approach and treat the problem by the instanton method, based on a multidimensional vibrational Hamiltonian. We have used this method successfully to calculate tunneling rates and splittings in molecules and complexes, not only for the zero-point level but also for excited levels.[7−11] In particular, it has proved to be capable of predicting the effect of vibrational excitation prior to the actual measurements.[11,12]

In section 2 we adapt formal expressions for these rate constants based on the approximate instanton method (AIM)[13] to the case of enzymatic CH-cleavage reactions. In section 3 we compare them with earlier expressions[5] derived from Fermi's golden rule. These two introductory sections provide the background for the semiempirical equations formulated in section 4, which allow direct application to kinetic data of reactions relevant to our purpose. This we show in section 6, where we apply them to eight CH-cleavage reactions to demonstrate that this yields further information about the mechanism of these reactions, including a test of the compatibility of the data with a single, rate-limiting tunneling step in the reaction sequence. It includes applications to mutants, as briefly discussed in section 5. In section 7 we compare the results, and in section 8 we draw some general conclusions.

2. INSTANTON APPROACH

This section reviews, extends, and where necessary corrects results we previously derived for application of the instanton method to proton transfer; it serves as an introduction to the equations in sections 4 and 5 for the applications reported in section 6. In the instanton approach, the set of all possible tunneling paths is represented by its dominant component, i.e., the instanton, defined as the path that represents a nontrivial extremum of the Euclidean action.[1] The tunneling rate constant is given by

$$k(T) = \mathscr{A}(T)e^{-S_I(T)} \tag{1}$$

where $S_I(T)$ is the instanton action (here and hereafter in units $\hbar$). To calculate this action, we use AIM[13] to create a multidimensional tunneling potential from calculated structures, energies, and force fields at points corresponding to the initial, final, and transition state of the system under discussion.[7] Using the normal modes of the transition-state configuration as our basis set, we first separate the tunneling mode, i.e., the reaction coordinate x corresponding to the imaginary frequency, from the transverse coordinates $\{y\}$. In lowest order we keep the transverse coordinates fixed to obtain the crude-adiabatic double-minimum potential $U_C(x)$. This potential is satisfactory only near the transition-state configuration. To obtain a satisfactory potential near the initial and final state, we subsequently introduce coupling between the tunneling mode and the transverse modes. Specifically, we limit ourselves to couplings linear in the y coordinates and neglect couplings between the latter coordinates. As argued in the Introduction, we assume the potential to be close to symmetric, which allows us to classify the normal modes according to the symmetry relative to the dividing plane of the reaction. The couplings are taken proportional to the displacements $\Delta y/\Delta x$ between the (roughly equivalent) equilibrium positions and the transition state. Since the coordinates are mass-weighted, the couplings are isotope-dependent. Only modes $\{y_s\}$ and modes $\{y_a\}$ that are, respectively, symmetric and antisymmetric, can be displaced. The multidimensional potential is formulated in terms of these two classes of displaced modes[7,13]

$$U(x,\{y\}) = U_A(x) + \frac{1}{2}\sum_a \omega_a^2(y_a - xC_a/\omega_a^2)^2 + \frac{1}{2}\sum_s \omega_s^2(y_s - x^2C_s/\omega_s^2)^2 \tag{2}$$

where $U_A(x)$ is the one-dimensional (1D) double-well adiabatic potential along the reaction coordinate, the transition state being at $x = 0$. The parameters $C_{a,s}$ are the coupling constants expressed in terms of the frequencies $\omega_{a,s}$ and the displacements Δx and $\Delta y_{a,s}$, which are derived, respectively, from the force fields and the geometries of the transition state and the stable configurations

$$C_a = \omega_a^2\Delta y_a/\Delta x, \qquad C_s = \omega_s^2\Delta y_s/(\Delta x)^2 \tag{3}$$

Only antisymmetric modes can be displaced between the initial and final configuration; the corresponding reorganization introduces a Franck−Condon factor into the expressions for the tunneling rate.

To proceed, we divide the transverse modes $\{y_{a,s}\}$ into "fast" and "slow" modes according to two criteria: their frequency relative to the mode with imaginary frequency and the strength of their coupling to this mode. As shown elsewhere,[7,13] this allows us to approximate the instanton action for this potential by an analytical expression of the general form

$$S_I(T) = \frac{S_I^0(T)}{1 + \sum_s \delta_s(T)} + \alpha \sum_a \delta_a(T) \quad (4)$$

where $S_I^0(T)$ is the instanton action for the 1D tunneling in the potential $U_A(x)$ with an effective mass μ_{eff} that comprises the effect of the fast modes; the coupling to the slow $y_{s,a}$ modes is represented by the correction terms $\delta_{s,a}(T)$. The parameter $\alpha < 1$ describes the effect of coupling to slow y_s modes on the tunneling distance. This representation of $S_I(T)$ shows that all the information about the tunneling in the absence of coupling, i.e., the mass of the tunneling particle and the shape of the potential, is in the corresponding 1D action $S_I^0(T)$, while the $\delta_{s,a}(T)$ terms are essentially independent of these parameters. On the other hand, $S_I^0(T) \simeq S_I^0(0)$ for the systems considered because at room temperature and below thermal excitation of the high-frequency CH-stretch modes has a minimal effect on the transfer rate. The temperature dependence is thus due mainly to the lower-frequency transverse modes representented by $\delta_{s,a}(T)$ and to the endothermicity ΔE_0, if any.

To obtain the 1D instanton action S_I^0 we can relate it to the classical action

$$S_I^0(E) = 2\int_{x_1}^{x_2} dx\{2\mu_{eff}[U_A(x) - E]\}^{1/2} \quad (5)$$

where $x_{1,2}$ are the turning points in the wells and $E = (1/2)\hbar\omega_0$ is the zero-point energy of the tunneling mode in the initial state. The mass-renormalization due to coupling to the fast modes is expected to be only weakly isotope-dependent; the effect on S_I^0 of substitution of D for H then follows from

$$\sqrt{\mu_{eff}^D/\mu_{eff}^H} \simeq \sqrt{\mu^D/\mu^H} = Q \quad (6)$$

We expect Q to be close to but slightly smaller than $\sqrt{2}$; in the numerical examples of section 6 we use the value 1.36, which is appropriate for CH and CD molecules.

The term $\alpha\Sigma_a\delta_a(T)$ is expected to exhibit only a small isotope dependence, which we will neglect. Its temperature dependence is given by

$$\delta_a(T) \simeq \delta_a(0)\tanh(\hbar\omega_a/4k_BT);\ \delta_a(0) = \Delta y_a^2\omega_a/\hbar \quad (7)$$

where in general $\omega_a \ll 4k_BT$ in the temperature region of interest. This means that we can approximate the hyperbolic tangents by their arguments to yield a term linear in the inverse temperature

$$\delta_a(T) \simeq \Delta y_a^2\omega_a^2/4k_BT \quad (8)$$

These modes we handle in the same way as the solvent modes treated by Marcus;[14] we assume that they reduce the transfer rate constant by a Boltzmann factor of the form $\exp[-(E_R + \Delta E_0)^2/4E_Rk_BT)]$, where E_R is a reorganization energy. Hereafter, the two terms ΔE_0 and E_R will be combined in the form of a single activation energy $\Delta E = (E_R + \Delta E_0)^2/4E_R$.

The term $\Sigma_s\delta_s(T)$ may be regarded as the relative contribution of the symmetric transverse modes to the transfer path. The contribution of a given mode will depend on its amplitude squared and thus on its vibrational quantum number, which implies

$$[\delta_s(T)]^{H,D} = [\delta_s(0)]^{H,D}\coth\frac{\hbar\omega_s}{4k_BT};\ [\delta_s(0)]^{H,D} = \frac{\omega_s^3\Delta y_s^2}{2\omega_0^{H,D}U_C} \quad (9)$$

In the adiabatic case where a hydrogen atom transfers between two carbon centers, there will be no hydrogen bonding, so that we may take $\hbar\omega_s \ll 4k_BT$ in the temperature region of interest. Then the hyperbolic cotangent can be approximated by its inverse argument as a result of which the $\Sigma_s\delta_s(T)$ reduces to a linear function of the temperature. This means that we can treat these low-frequency symmetric modes collectively as a single mode, thus eliminating the summation over s. In the nonadiabatic case, electron transfer creates ionic configurations, so that the moving proton will be subject to hydrogen bonding; we then expect a single transverse mode, namely, the hydrogen-bond stretching mode between the donor and acceptor centers, usually referred to as the "promoting" or "gating" mode, to dominate the coupling to the tunneling mode. In this case, we replace the sum in eq 4 by a single term $\delta_s(T) = \delta_s(0)\coth(\hbar\omega_s/4k_BT)$ associated with this mode. This means that we can now formally combine the results for adiabatic and nonadiabatic transfer into a single expression

$$S_I^{H,D}(T) \simeq \frac{[S_I^0(0)]^{H,D}}{1 + [\delta_s(0)]^{H,D}\coth(\hbar\omega_s/4k_BT)} + \frac{\Delta E}{k_BT} \quad (10)$$

in which the isotope-dependent and temperature-dependent factors are clearly separated.

Thus, the first term in eq 10 reduces effectively to the solution of a 2D Hamiltonian. Benderskii et al.[15] have studied this 2D Hamiltonian for a symmetric collinear three-atom reaction X−H···Y → X···H−Y of the type "heavy−light−heavy", where X = Y. Assuming harmonic forces along the XH bond and between X and Y, and introducing the coordinates x and y of the XH and XY oscillators, respectively, defined relative to the center of mass, we can reduce eq 2 to

$$H(x,y) = \frac{1}{2}\mu_0\dot{x}^2 + \frac{1}{2}\mu_s\dot{y}^2 + U_{1D}(x;y) + \frac{1}{2}\mu_s\omega_s^2y^2 \quad (11)$$

where $x = x^H - (x^X + x^Y)/2$, $y = (x^X - x^Y) - 2x_0$, $\mu_0 = 2m^Hm^X/(m^H + 2m^X)$, $\mu_s = m^X/2$, $x_0 = r_0/2$, i.e. half the (equilibrium) transfer distance, and ω_s is the frequency corresponding to the harmonic XY force field; the 1D potential

$$U_{1D}(x;y) = U_0(|x| - \bar{x})^2 \quad (12)$$

is a symmetric double-minimum potential that depends parametrically on the heavy-atom coordinate y through $\bar{x} = x_0 + y/2$, and $U_0 = \mu_0\omega_0^2x_0^2/2$ is the (equilibrium) barrier height, ω_0 being the frequency corresponding to the harmonic XH force field. It consists of two crossing parabolas truncated after the crossing to form a barrier whose top is a singular point. An alternative potential without a singularity is the quartic potential

$$U_{1D}(x;y) = U_0(x^2 - \bar{x}^2)^2 \quad (13)$$

with $U_0 = \mu_0\omega_0x_0^2/8$ and $\bar{x} = [x_0(x_0 + y/2)]^{1/2}$.

Our aim is to express $S_I(T)$ for this reaction in the generic form represented by the first term of eq 4, viz.

$$S_I(T) = \frac{S_I^0(T)}{1 + \delta_s(T)} \quad (14)$$

dx.doi.org/10.1021/jp2022117 |J. Phys. Chem. B 2011, 115, 7679–7692

To achieve this, we use the 2D instanton solutions found by Benderskii et al.[15] for these two model double-minimum potentials. The solutions, including the rate constant in eq 1, describe incoherent tunneling provided that the decay width of the energy levels is large enough. These solutions can be expressed in terms of the parameters

$$A_z = \gamma^2/4\tilde{\omega}_s, \qquad B_z = \gamma^2/2\tilde{\omega}_s{}^2 \tag{15}$$

where the dimensionless parameter $\gamma = (\mu_0/\mu_s)^{1/2}$ defines the coupling strength, and $\tilde{\omega}_s = \omega_s/\Omega$, the scaling frequency Ω being defined by $U_0 = \mu_0 x_0^2 \Omega^2$. For the crossing-parabola potential defined by eq 12, the 2D Hamiltonian can be diagonalized analytically by rotation of the vector $\{x,y\}$ over an angle ϕ defined by the relations

$$\tan\phi = \sqrt{\frac{\Omega_+^2 - \omega_0^2}{\omega_0^2 - \Omega_-^2}};$$

$$\Omega_\pm = \Omega\left[1 + \omega_p^2/2 \pm \sqrt{(1-\omega_p^2/2)^2 + \gamma^2}\right]^{1/2};$$

$$\omega_p = \sqrt{\tilde{\omega}^2 + \gamma^2/2} \tag{16}$$

The instanton solution then takes the form

$$S_I(T) = \frac{\mu_0 r_0^2/2}{\Omega_+^{-1}\cos^2\phi\,\coth(\hbar\Omega_+/4k_BT) + \Omega_-^{-1}\sin^2\phi\,\coth(\hbar\Omega_-/4k_BT)} \tag{17}$$

In our case, where hydrogen is exchanged between two much heavier atoms, the coupling is weak, so that expansion of the analytical expression in terms of γ^2 converges rapidly to eq 14 with

$$S_I^0(T) \simeq S_I^0(0), \qquad \delta_s(T) = A_z\sqrt{2}\,\coth\frac{\hbar\omega_s}{4k_BT} \tag{18}$$

leading to[16]

$$S_I(T) \simeq \frac{\frac{1}{2}\mu_0\omega_0 r_0^2}{1 + \frac{1}{4}(\mu_0\omega_0/\mu_s\omega_s)\coth(\hbar\omega_s/4k_BT)} \tag{19}$$

For the quartic potential, the Hamiltonian given by eq 11 cannot be diagonalized exactly. Depending on the parameter values and the temperature, different approximate treatments apply.[15] In our case, the hydrogen motion in the well is fast compared to the heavy atom motion, and the coupling between the two motions is weak, which corresponds to the sudden (or "fast-flip") approximation. The heavy-atom motion will then promote tunneling by reducing the tunneling distance r_0 by a factor $q_0 < 1$. For temperatures in the range of interest $\hbar\omega_s/4k_B \le T \ll \hbar\omega_0/4k_B$, the instanton action obtained in ref 15 can be expressed in the form

$$S_I(T) = S_I^0(0)q_0^3 + \frac{1}{B_z}\frac{U_0}{k_BT}(q_0^2-1)^2,\ S_I^0(0) = \frac{1}{3}\mu_0\omega_0 r_0^2 \tag{20}$$

where $S_I^0(0)$ is the corresponding 1D instanton action at zero temperature and

$$q_0 = \sqrt{1+\theta^2} - \theta, \qquad \theta = 2\sqrt{2}A_z\frac{k_BT}{\hbar\omega_s} \tag{21}$$

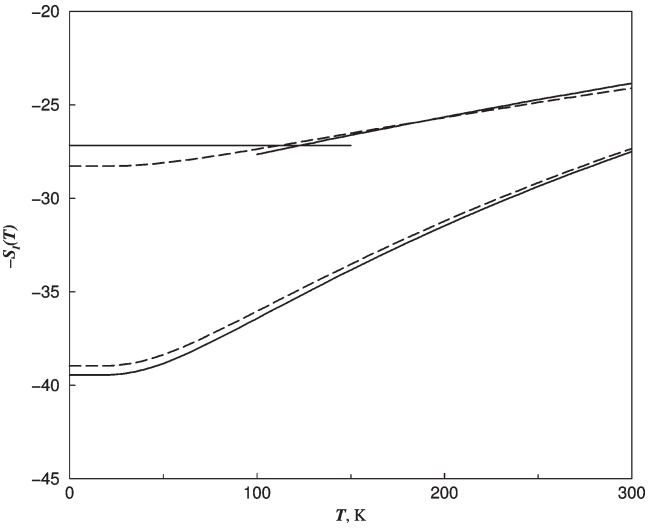

Figure 1. Comparison of the exact instanton solutions (solid lines) and the generic solutions (dashed lines) represented by eq 24 for the quartic potential (top) and by eq 19 for crossing parabolas (bottom). For consistency, the latter includes the instanton solution in the low-temperature range.[15] Parameter values: $\mu_0 = 1$ (in atomic units), $r_0 = 1.0$ Å, $\omega_0 = 3000$ cm^{-1}, $\mu_s/m_0 = 25$, $\omega_s = 200$ cm^{-1}.

Note that these expressions differ slightly from those we reported earlier.[17] At room temperature or below we obtain $\theta \simeq (1/2)\delta_s(T)$. Since the coupling is assumed to be weak, $\theta \ll 1$ can be used as an expansion parameter for $S_I(T)$. Terminating the expansion after terms of the order θ^2 and using the identity

$$1 - X \equiv \frac{1}{1 + X/(1-X)},$$
$$X = (3/4)\delta_s(T)[1 - \delta_s(T)/2] \tag{22}$$

we obtain[17]

$$S_I(T) \simeq \frac{S_I^0(0)}{1 + \Gamma\delta_s(T)}, \qquad \Gamma = (3/4)[1 + \delta_s(T)/4] \tag{23}$$

Thus, for weak coupling we have for the quartic potential $\Gamma\delta_s(T) = (3/4)A_z\sqrt{2}\,\coth(\hbar\omega_s/4k_BT)$. For the curvature at the bottom of the wells, we have $\omega_0 = 2\sqrt{2}\Omega$, a value close to the results obtained quantum-chemically for hydrogen-bonded systems. Using these results together with eq 15, we obtain

$$S_I(T) \simeq \frac{\frac{1}{3}\mu_0\omega_0 r_0^2}{1 + \frac{3}{32}(\mu_0\omega_0/\mu_s\omega_s)\coth(\hbar\omega_s/4k_BT)} \tag{24}$$

an equation of the same form as eq 19 but with different numerical coefficients. A comparison of eqs 19 and 24 with the exact instanton solutions for the two types of potential is shown in Figure 1.

These calculations show that eq 4 for the instanton action $S_I(T)$ is (approximately) valid for a wide range of double-minimum potentials. The main advantage of this representation, which forms the basis of the Approximate Instanton Method as implemented in the DOIT 2.0 program,[18,19] is that no explicit knowledge of the instanton trajectory is required for the evaluation of tunneling rate constants. The method has been applied successfully to a variety of tunneling splittings and rates.[8−13]

3. COMPARISON WITH THE GOLDEN RULE APPROACH

In this section, we compare the instanton expressions with expressions derived earlier[5] with Fermi's golden rule in which the rate of transfer is proportional to the square of the coupling matrix element between an initial state Ψ_i and a final state Ψ_f

$$k(T) = \frac{2\pi}{\hbar}|<\Psi_f|V|\Psi_i>|^2\delta(E_f - E_i) \quad (25)$$

where V is a coupling operator and the delta function is required for energy conservation. We split the Hamiltonian H of the system into a zeroth-order part $H-V$ with eigenfunctions Ψ_i and Ψ_f and a coupling V such that the eigenfunctions are products of electronic and vibrational wave functions, denoted by Φ and Λ, respectively, and the coupling is independent of the latter. Then we separate Λ in a strongly displaced tunneling mode λ and a set of lower-frequency transverse modes Λ', that remain essentially unaltered between both states. We further assume that the frequency of the tunneling mode is much larger than the thermal energy k_BT and than the endothermicity ΔE_0, and we interpret the delta function in eq 25 as a density of (final) states $\rho(E_f)$. For adiabatic transfer where $\Phi_i = \Phi_f$, we then obtain

$$\ln k(T) = L_A + \ln(|<\Lambda'|s_{00}|\Lambda'>|^2) - \Delta E_0/k_BT \quad (26)$$

where

$$L_A = \ln\left[\frac{2\pi}{\hbar}|<\Phi_f^I|V|\Phi_i^I>|^2\rho(E_f)\right] \quad (27)$$

lumps together terms that are isotope- and temperature-independent.

Since we assume that the transfer is close to thermoneutral, at room temperature or below, both CH-stretching vibrations will be in the ground state $v = 0$. In the harmonic approximation, their squared overlap integral will be $s_{00}^2 = \exp[(r_i - r_f)^2/2a_0^2]$, where $a_0 = (\hbar/\mu_0\omega_0)^{1/2}$ is the zero-point amplitude, μ_0 and ω_0 being the (averaged) mass and frequency of the two CH oscillators. The skeletal vibrations that modulate $r_i - r_f$ are approximated by a 1D effective mode, represented by a harmonic oscillator $\lambda(R)$, which may be formally identified with the C···H···C stretching mode with R parallel to the tunneling coordinate r so that $R = r + 2b$, where b is the CH bond length. The squared amplitude of this mode is given by

$$a_s^2(T) = a_s^2(0)\coth(\hbar\omega_s/2k_BT) \quad (28)$$

where $a_s(0) = (\hbar/\mu_s\omega_s)^{1/2}$, μ_s and ω_s being the effective mass and frequency, respectively.

If there is no hydrogen bonding, we can approximate the zero-point wave functions in the wells by harmonic-oscillator functions. To evaluate the two-dimensional overlap integral

$$S_{00}(T)| = <\lambda(R)|s_{00}(R-2b)|\lambda(R)> \quad (29)$$

analytically, we consider two limiting cases. In the limit where $\hbar\Omega \ll k_BT$ we replace the R-oscillations because they are slow compared to the r-oscillations, by a distribution $P(R,T)$ of R-values. The simplest assumption we can make is that this distribution is normal, i.e., Gaussian

$$P(R,T) = \frac{\exp\{-(R-R_0)^2/a_s^2(T)\}}{\sqrt{\pi}a_s(T)} \quad (30)$$

This approximation should be adequate when the effective mode represents the result of small contributions of many low-frequency skeletal modes. Multiplying $P(R,T)$ by s_{00}^2 and integrating over R, we obtain

$$\ln|S_{00}(T)|^2 \rightarrow -\frac{r_0^2}{2a_0^2 + a_s^2(T)};\ k_BT \gg \hbar\omega_s \quad (31)$$

This equation was used in our earlier publication.[5] However, there is an alternative limit that applies for low temperatures where the frequency ω_s of the effective mode is large compared to the thermal energy; $\lambda(R)$ will then effectively reduce to the zero-point wave function, so that, in the harmonic approximation, we obtain, with $s_{00} = \exp(-(R-2b)^2/4a_0^2)$

$$\lim_{T\rightarrow 0}\ln|S_{00}(T)|^2 = -\frac{r_0^2}{2a_0^2 + \frac{1}{2}a_s^2(0)} \quad (32)$$

We can combine eqs 28 and 31 by rewriting them in the form

$$\ln|S_{00}(T)|^2 = -\frac{r_0^2}{2a_0^2 + \frac{1}{2}a_s^2(0)\coth(\hbar\omega_s/4k_BT)} \quad (33)$$

This equation is similar to eq 19 derived by the instanton method. The nature of the approximations used suggests that it is only valid for deep harmonic wells, i.e., for adiabatic hydrogen transfer between two carbon centers.

To generalize this equation to nonadiabatic transfer between a carbon and an oxygen center, we dropped the Condon approximation and introduced anharmonic wells in a heuristic manner by replacing the zero-point amplitude a_0 by an effective amplitude $a_{eff} > a_0$. We introduced couplings linear in the tunneling coordinate, which are expected to be weak in this case. In the notation of eqs 19 and 24, this means that we introduced a single empirical coefficient to reduce the terms in the numerator and the denominator of eq 19. While this leads almost to eq 24, the fact that this coefficient is essentially arbitrary reduces its usefulness. The main value of this approach is its transparency, which may provide a more intuitive grasp of the instanton results. In the instanton approach there are two different coefficients, both of which are derived from the shape of the transfer potential, and this potential is chosen on the basis of results previously obtained for hydrogen-bonded systems, as shown in section 2.

4. DATA ANALYSIS

The simple form of eqs 19 and 24 renders them useful for data analysis even when the required quantum-chemical input data are not readily available, namely, in the form of semiempirical relations that can be suitably parametrized. The corresponding rate constants for H and D transfer can be expressed in the form

$$\ln k^H(T) = L - \frac{S_1^0(0)}{1 + \sum_s \delta_s(T)} + \alpha\sum_a \delta_a(T);$$
$$\ln k^D(T) = L - \frac{S_1^0(0)Q}{1 + Q\sum_s \delta_s(T)} + \alpha\sum_a \delta_a(T) \quad (34)$$

where L represents the pre-exponential term in eq 1, which we suppose to be temperature independent and the same for both isotopes. The two equations differ only by factors Q, which may be treated as a known parameter. Using the derivation

in the preceding sections, we rewrite these equations in parametrized form as

$$\ln k^{H}(T) = L - \frac{\rho}{1+z(T)} - \frac{\Delta E}{k_B T};$$
$$\ln k^{D}(T) = L - \frac{\rho Q}{1+z(T)Q} - \frac{\Delta E}{k_B T} \quad (35)$$

where

$$\rho = c_1 \mu_0 \omega_0 r_0^2; \qquad z(T) = c_2 \frac{\mu_0 \omega_0}{\mu_s \omega_s} \coth \frac{\hbar \omega_s}{4 k_B T} \quad (36)$$

For adiabatic transitions of the type considered, we have according to eq 19: $c_1 = 1/2$, $c_2 = 1/4$. For nonadiabatic transitions, we have according to eq 24: $c_1 = 1/3$, $c_2 = 3/32$. This means that the parameters ρ and $z(T)$ apply to adiabatic as well as nonadiabatic transfers and thus to a wide variety of double-minimum potentials. What varies is the interpretation of these model parameters in terms of physical parameters, such as r_0 and $\mu_s \omega_s$.

The isotope dependence of the rate constant is expressed by η, the ratio of the H and D transfer rate constants. From eq 35 it follows that

$$\ln \eta = \frac{\rho(Q-1)}{[1+z(T)][1+z(T)Q]} \quad (37)$$

The temperature dependence of the rate constants is expressed by the effective activation energies $E_a^{H,D}$ obtained by differentiation of eqs 35 with respect to the inverse temperature

$$\frac{E_a^H}{k_B T} = -\frac{d \ln k^H(T)}{d \ln T^{-1}} = \frac{\rho z(T) F(T)}{[1+z(T)]^2} + \frac{\Delta E}{k_B T}$$
$$\frac{E_a^D}{k_B T} = -\frac{d \ln k^D(T)}{d \ln T^{-1}} = \frac{\rho Q^2 z(T) F(T)}{[1+z(T)Q]^2} + \frac{\Delta E}{k_B T} \quad (38)$$

where

$$F(T) = \frac{\hbar \omega_s}{4 k_B T}\left(\coth \frac{\hbar \omega_s}{4 k_B T} - \tanh \frac{\hbar \omega_s}{4 k_B T}\right) \quad (39)$$

varies smoothly from 0 to 1 as a function of temperature. It can be set equal to 1 when $\hbar \omega_s \ll 4 k_B T$, i.e., when the mobile proton is not hydrogen bonded.

For practical applications, it is useful to combine these equations with eq 37 and rewrite them in the form

$$\frac{E_a^H - \Delta E}{k_B T} = \frac{z(T) F(T) \ln \eta}{Q-1} \cdot \frac{1+z(T)Q}{1+z(T)} \quad (40)$$

$$\frac{E_a^D - \Delta E}{k_B T} = \frac{z(T) F(T) \ln \eta}{Q-1} \cdot \frac{[1+z(T)]Q^2}{1+z(T)Q} \quad (41)$$

or alternatively

$$\frac{E_a^D - \Delta E}{E_a^H - \Delta E} = \left\{\frac{[1+z(T)]Q}{1+z(T)Q}\right\}^2 \quad (42)$$

$$\frac{\Delta E_a}{k_B T} \equiv \frac{E_a^D - E_a^H}{k_B T} = z(T) F(T) \frac{1+Q+2z(T)Q}{[1+z(T)][1+z(T)Q]} \ln \eta \quad (43)$$

This last equation, which does not involve ΔE, is the only one available when the KIE is obtained from product analysis. Although eqs 42 and 43 are formally equivalent to eqs 40 and 41, they tend to be more sensitive to the accuracy of the input data and should not be used as a shortcut. If the H and D rates are measured separately, eqs 40 and 41 both contain three fitting parameters: $z(T)$, ΔE, and $F(T)$. Of these, $F(T)$ depends only on ω_s and can be set equal to 1 when $\hbar \omega_s \ll 4 k_B T$, i.e., for adiabatic transfer. Variation within the range 0.9−1 should be satisfactory for nonadiabatic transitions near room temperature. For typical enzymatic reactions, we expect ΔE to be small, in which case the similarity of the $z(T)$ values obtained from eqs 40 and 41 provides a test for the applicability of the model. Other tests follow from the constraints

$$\frac{E_a^H - \Delta E}{k_B T} \le \frac{\rho F(T)}{4}; \qquad \frac{E_a^D - \Delta E}{k_B T} \le \frac{\rho F(T) Q}{4} \quad (44)$$

and

$$\frac{E_a^D}{E_a^H} \le Q^2 < 2, \qquad \frac{\Delta E_a}{k_B T} < 2 \ln \eta \quad (45)$$

which are easily derived from eqs 42 and 43. Once a satisfactory value for $z(T)$ is obtained, we can calculate ρ and thus the transfer distance r_0 from eq 36, which will provide direct information on the mechanism of the transfer.

For carbon and oxygen centers, the van der Waals radii of the atomic centers between which the transfer occurs amount to about 2.0 and 1.4 Å, respectively, with CH and OH bond lengths of about 1.08 and 0.97 Å. For the mass and frequency of the CH/OH oscillators, we use $\mu_0 = 1$ in atomic units and $\omega_0 = 3000\ \mathrm{cm}^{-1}$. For adiabatic transfer, substitution in eq 36 with $r_0 \sim 1.8$ Å leads to $\rho \sim 150$. For nonadiabatic transfer, there will be hydrogen bonding, which will shorten the transfer distance. In the absence of specific information about this bonding, we restrict ourselves to the estimates $r_0 \sim 1$ Å and $\rho < 40$; these values are sufficiently different from those for adiabatic transfer to distinguish between the two mechanisms. Since $F(T)$ depends only on ω_s, it can be combined with the derived value of $z(T)$ to yield a value for the product $\mu_s \omega_s$. These numerical estimates put additional constraint on the solutions obtained from eqs 40−43. Armed with these results, we can find out whether a given kinetic data set is compatible with a single tunneling step and, if so, which transfer mechanism is operative and which physical parameter values apply. In section 6 this approach is put to the test.

5. MUTANTS

Experimental studies of enzymatic reactions occasionally make use of mutants in which one amino acid at or near the active site is replaced by another. If such a substitution affects the kinetics, it indicates that the amino acid is participating in some aspect of the transfer; it may affect the transfer distance, the transverse modes involved, and/or the energetics of the reaction. It is difficult to treat theoretically since, in principle, not only the vibrational but also the electronic matrix elements are affected. In the present context, we will only consider mutations for which it may be reasonably assumed that the electronic matrix elements remain invariant. In that case, only three of the model parameters are affected, namely, ρ, $z(T)$, and ΔE. In addition to eq 35, we now have a new set of the same form but with these three parameters along with the rate constants labeled by an index, say 1, for the mutant. Consider

the pair

$$\ln k^{H}(T) = L - \frac{\rho}{1+z(T)} - \frac{\Delta E}{k_B T};$$
$$\ln k_1^{H}(T) = L - \frac{\rho_1}{1+z_1(T)} - \frac{\Delta E_1}{k_B T} \quad (46)$$

Once the three model parameters for each species are derived from their isotope and temperature dependence, these equations and their companion equations for deuterium transfer allow an independent check on the parameter values since the absolute values of the rate constants are not used in these derivations. There is also an independent physical test since an increase of the distance parameter ρ in the mutant relative to the wild-type enzyme is expected to be accompanied by an increase of the promoting-mode contribution, given by $z(T)$. These points are elaborated in section 6.4 where several examples are analyzed.

6. APPLICATIONS

In this section, we use the equations of section 4 to analyze experimental data, usually provided in the form of a series of H and D transfer rate constants measured in a relatively narrow temperature interval. In all cases considered here, the reported data give rise to linear Arrhenius plots, but this is not necessary for the analysis since slopes are needed at one temperature only. For linear plots we will choose the midpoint of the temperature interval used. The transfer rate constants are usually measured as the initial rate of product formation under excess substrate conditions, based on the Michaelis−Menten equation, which in its simplest form is given by

$$k_{t\to 0} = k_{cat}[SH]/([SH] + K_M) \quad (47)$$

where [SH] is the substrate concentration and $K_M = (k_{-1} + k_{cat})/k_1$ is the Michaelis constant, k_1 and k_{-1} being the association and dissociation rate constants, respectively, of the reactive complex formed by enzyme and substrate; k_{cat} is the hydrogen transfer rate constant. The validity of eq 47 does not prove, however, that tunneling is the unique rate-limiting step. Hence it is useful to have a theoretical method to test this assumption.

6.1. Coenzyme B_{12}. We first consider a CH-cleavage reaction that is generally accepted to be adiabatic, namely, hydrogen transfer catalyzed by coenzyme B_{12}, in which a cobalt-centered complex (Cbl) releases the ligand 5′-deoxyadenosyl (Ado) in the form of a free radical. This radical abstracts a hydrogen atom from a CH bond of the substrate, a process characterized by a large and strongly temperature-dependent KIE. The hydrogen abstraction step in methylmalonyl-coenzyme A mutase (MMCoAM) has been studied by Chowdhury and Banerjee[20] in the range 278−293 K. The kinetic data at T = 286 K relevant for our purpose are: $\ln \eta = 3.8 \pm 0.4$; $E_a^H/k_BT = 31.0 \pm 1.8$; $E_a^D/k_BT = 37.6 \pm 2.2$. In view of the magnitude of the KIE we can safely assume that tunneling dominates both H and D transfer. To start the analysis, we tentatively assume that transfer between a methyl radical and a methyl group is roughly thermoneutral and involves no substantial reorganization, so that $\Delta E \sim 0$. Since no hydrogen bonding is expected, we can set $F(T) \sim 1$. Using eqs 40 and 41 we obtain $z(286) = 2.34$ with $\rho = 148$ and $z(286) = 2.42$ with $\rho = 155$, respectively. The results for H and D transfer are thus mutually consistent, and the ρ values lead to a transfer distance $r_0 = 1.83$ Å, which is well within the estimated range for adiabatic transfer. It also agrees well with the value of 1.88 Å measured by Doba et al.[21] for hydrogen abstraction by a methyl radical from the methyl group of methanol in a methanol glass. The satisfactory fit of eqs 35 and 37 to the data shown in Figure 2 implies that in the region of the measurements $F(286) \simeq 1$ and thus $\omega_s \ll 4k_BT$. This is confirmed by the weak curvature of the Arrhenius plots and more directly by the values of the combination of ω_s (in cm^{-1}) and μ_s (in atomic units) derived from eq 36, e.g., 70 and 50 or 50 and 100.

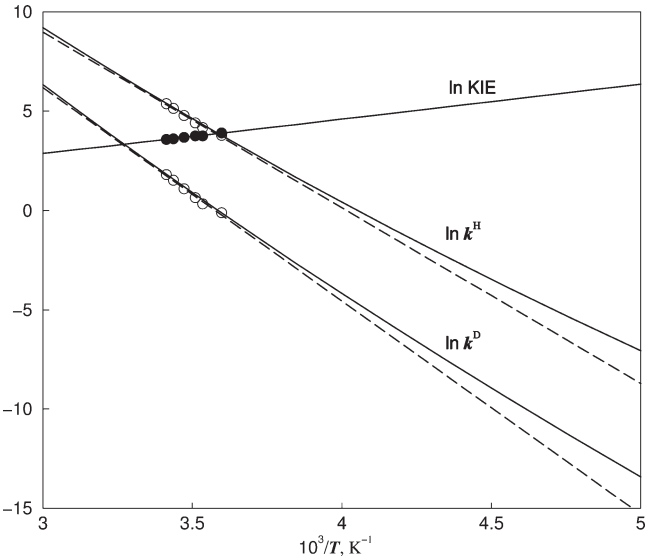

Figure 2. Logarithmic plot of the rate constants and KIE as a function of the inverse temperature for the hydrogen abstraction step in methylmalonyl-coenzyme A mutase (MMCoAM)[20] discussed in section 6.1, showing the strong temperature dependence of the KIE typical for abstraction by free radicals. Open and closed circles refer to observed[20] rate constants for H/D transfer and the corresponding KIE, respectively. The solid lines are calculated from eqs 35 and 37 with parameter values deduced from eqs 40 and 41. The broken lines are standard linear Arrhenius plots.

Hence the results for this reaction agree with the accepted adiabatic transfer mechanism and support the assumptions $\Delta E \sim 0$ and $F(T) \sim 1$. The relatively large value of $z(T)$ indicates that the transfer is strongly supported by excited skeletal vibrations. Since the adiabatic mechanism does not involve hydrogen bonding, this support will be distributed over a number of low-frequency modes whose amplitudes are strongly enhanced by thermal excitation at room temperature. The observation that an essentially harmonic model fits the data is in agreement with the notion that in this system the well is very deep and hence harmonic near the bottom. As a result a simple golden rule treatment can replace the instanton treatment for this system.

A similar reaction but without the enzyme has been studied by Doll and Finke,[22] whose substrate was the solvent ethylene glycol; the relevant kinetic data for neopentyl replacing Ado (the Ado reaction required too high a temperature to justify use of the present model) derived from product distributions are $\ln \eta(292) = 3.6$ and $\Delta E_a/k_BT = 5.3$. If we apply eq 43 with $F(T) \sim 1$, we obtain $z(292) = 2.40$; substitution in eq 36 yields $\rho = 153$. The results are thus the same as those obtained above for MMCoAM.

6.2. Galactose Oxidase. A second enzyme that presumably cleaves CH bonds adiabatically is galactose oxidase (GalOx), a radical-coupled enzyme containing a free radical coordinated to

copper. It catalyzes two-electron oxidation of alcohols to aldehydes. The large KIE suggests that abstraction of an H atom, presumably by a tyrosyl radical, is rate-limiting. Whittaker et al.[23] have carried out measurements with deuterium-labeled substrates that appear to support this mechanism. Specifically, they have measured the isotope dependence of the KIE as a function of temperature in the interval 277−318 K. From the Arrhenius-type plot of Figure 7 of ref 23, we obtain the values ln $\eta = 2.8$ and $\Delta E_a = 4.2$ at 298 K: a modest isotope effect that is strongly temperature-dependent, a pattern that resembles, at a lower level, that observed in coenzyme B_{12}. Substitution of these data in eq 43 yields $z(T) = 2.6$ with $\rho = 130$, corresponding to a transfer distance $r_0 = 1.7$ Å, a value similar to those obtained in section 6.1, in agreement with the presumed free radical mechanism. However, the numerical accuracy of these results suffers from the fact that for large $z(T)$ eq 43 tends to become unstable. This situation arises for relatively small KIE values, i.e., when over-barrier contributions tend to become important.

6.3. Benzylic Hydroxylation by Aromatic Amino Hydroxylases. Phenylalanine hydroxylase (PheH), which contains a nonheme iron ion, belongs to a family of enzymes that catalyze hydroxylation of the side chain of phenylalanine and other aromatic amino acids. It inserts an oxygen atom taken from an O_2 molecule into an aromatic CH bond and uses tetrahydropterin as a source of electrons to reduce the remaining oxygen atom. The mechanism of the reaction, which is not yet fully understood, has been reviewed by Fitzpatrick.[24] It involves a hydrogen abstraction step, which for some of the enzymes appears to be rate-limiting, as indicated by the observation of a KIE of about 10 at 298 K. The mechanism of the abstraction reaction is not known, but it has been plausibly suggested that it involves an Fe(IV)O intermediate. As Bassan et al.[25] have shown in a recent theoretical study, this leaves open the question whether the reaction follows an ionic or a free-radical pathway, i.e., whether a proton or a hydrogen atom is abstracted.

Using product analysis Pavon and Fitzpatrick[26] measured the temperature dependence of the KIE of the abstraction step in the transformation of 4-CH_3-phenylalanine into 4-$OHCH_3$-phenylalanine in the range 280−330 K. They compared four enzymes that attack the 3- and 4-positions of the aromatic ring, namely, PheH, its mutant Δ117PheH, tyrosine hydroxylase (TyrH), and a mutant of tryptophan hydroxylase ($TrpH_{102-106}$); the mutants lack the N-terminal regulatory domains. PheH was found to favor the 4-position, while the other enzymes were less specific. The observed KIEs increased with decreasing temperature, and the Arrhenius plots yielded frequency factor ratios A_H/A_D in the range 0.1−0.2. The reported values for the primary KIE vary from 12 to 14 with an average uncertainty of 0.5. These values are clearly too small to ascertain that tunneling is the dominant transfer mechanism. The values for ΔE_a vary from 2.4 to 2.9 kcal/mol or 4.0−4.9 k_BT with an average uncertainty of 0.3 kcal/mol and are similar to those for GalOx discussed in the previous subsection; they indicate that the reaction is adiabatic and involves hydrogen abstraction by a free radical. However, the numerical instability of eq 43 for the corresponding large $z(T)$ values prevents a reliable analysis. Substitution of the values ln $\eta = 2.5$ and $\Delta E_a/k_BT = 4.0$ for PheH and its mutant in eq 43 yields $z(T) = 3.5$ and $\rho = 180$, corresponding to a transfer distance of 2.0 Å. For the other enzymes the calculation yields $z(T)$ values of the order of 10, indicating that skeletal motion rather then tunneling dominates the transfer. To the extent that tunneling contributes, it appears to be via a free radical mechanism. However, as indicated by this and the previous example, the analysis tends to become uncertain for KIE values below 20, especially if measured indirectly by product analysis.

6.4. Lipoxygenase-1. Klinman and co-workers[27,28] carried out an extensive study of hydrogen transfer in linoleic acid catalyzed by soybean lipoxygenase-1 (SLO1). The active site in this enzyme contains a six-coordinated iron ion that alternates between Fe(III) and Fe(II) during the catalytic cycle in which an electron is abstracted from a CH bond of the C-11 methylene group of linoleic acid. This weakens the bond sufficiently to allow transfer of the proton to an OH group coordinated to the iron ion. Since the electron and the proton involved in the CH-bond cleavage move to different atoms, the reaction is a nonadiabatic process. Experimentally, the progress of the reaction is monitored by the formation of an intermediate peroxide after proton transfer. The reported results include rate constants k_{cat} and Michaelis constants K_M as defined in eq 47 for hydrogen and deuterium transfer at up to 10 temperatures in the range 278−323 K for the wild-type (WT) enzyme and six mutants. The mutants differ from the WT enzyme in the shape and size of the alkyl part of one amino acid residue. For a detailed description of the reaction and the location and identification of the mutant amino acid residues, we refer to the original papers.[27,28] For clarity we have replotted the results in an earlier, preliminary study.[5] The pertinent experimental data derived from these plots are collected in Table 1, along with very similar results that were obtained recently by Jacquot et al.[29] for the same reaction in the range 278−308 K with linoleic acid replaced by arachidonic acid.

The resulting set of kinetic data on seven closely related enzymes has been analyzed by the original authors in terms of a two-oscillator model treated numerically. To a first approximation, this model, based on the Condon approximation, is similar to one that we introduced many years ago and applied more recently to the present system.[5] It is not strictly valid for nonadiabatic transfer, where the coupling between the vibrational manifolds of the initial and final state is a function of vibrational coordinates. The oscillators, which comprise a tunneling mode and a promoting mode, were represented by a Morse oscillator and a harmonic oscillator, respectively, or by two Morse oscillators, coupled through their displacements.

Our present analysis starts with the WT enzyme. Since the mechanism is known to be nonadiabatic, we set $F(T) = 0.9$ at room temperature, corresponding to a promoting-mode frequency of about 300 cm^{-1}. In view of the small activation energies, we further set $\Delta E \simeq 0$. Using eqs 40 and 41 with input parameters from Table 1 measured at $T = 298$ K, we obtain from the H- and D-transfer data, respectively, $z(T) = 0.24$, $\rho = 20$ and $z(T) = 0.28$, $\rho = 22$ as listed in the final columns of Table 1. The agreement between these pairs of values is not perfect but well within the experimental error limits. The average value for the transfer distance is thus $r_0 = 0.83 \pm 0.02$ Å. The results in ref 29 give rise to an average transfer distance $r_0 = 0.85$ Å, also shown in Table 1. The assumed promoting-mode frequency would imply an effective mass $\mu_s = 21$ in atomic units. An increase of ω_s to 400 cm^{-1} would reduce μ_s to 12. Introduction of a nonzero value of ΔE would increase the error of the fit and decrease the transfer distance.

The two mutants I553A and I553L in Table 1 have essentially the same rate constants both for H and for D transfer as the WT enzyme in the center of the temperature interval studied, and thus the same KIE at 298 K, but exhibit different activation energies. Applying the above procedure to these mutants we get

Table 1. Columns 2−5, Rows 1−7, Are Rate Constants k^H (in s^{-1}) and Activation Energies E_a[a]) of Soybean Lipoxygenase-1 and Six Mutants Calculated by Linear Regression from the Kinetic Data Reported As Supporting Information in Refs 27 and 28 and Row 8 in Ref 29, and Columns 6 and 7 Are Kinetic Model Parameters Derived from These Data

enzyme	ln k^H	ln η	E_a^H/k_BT	E_a^D/k_BT	H: $z(T)//\rho$	D: $z(T)//\rho$
Linoleic/SLO1	5.7 ± 0.2	4.4 ± 0.5	2.8 ± 0.5	5.3 ± 1.2	0.24//20	0.28//22
Mutant I553A	5.7 ± 0.1	4.5 ± 0.5	3.3 ± 0.7	8.6 ± 1.0	0.27//22	0.46//30
Mutant I553L	5.8 ± 0.1	4.5 ± 0.4	0.7 ± 1.2	6.7 ± 0.5	0.06//14	0.35//25
Mutant I553 V	4.3 ± 0.2	4.3 ± 0.6	4.1 ± 0.9	8.3 ± 1.1	0.35//24	0.47//29
Mutant I553G	4.1 ± 0.1	5.3 ± 0.4	0.0 ± 0.7	7.3 ± 0.7	-//-	0.32//28
Mutant L546A	0.4 ± 0.2	4.8 ± 0.6	5.6 ± 0.4	9.3 ± 0.8	0.42//30	0.47//32
Mutant L754A	− 1.7 ± 0.3	4.6 ± 0.6	6.2 ± 0.8	8.9 ± 1.7	0.48//31	0.47//31
Arachid/SLO1	6.1	4.6	2.4	7.0	0.18//19	0.32//24

[a] In units of the thermal energy at T = 298 K.

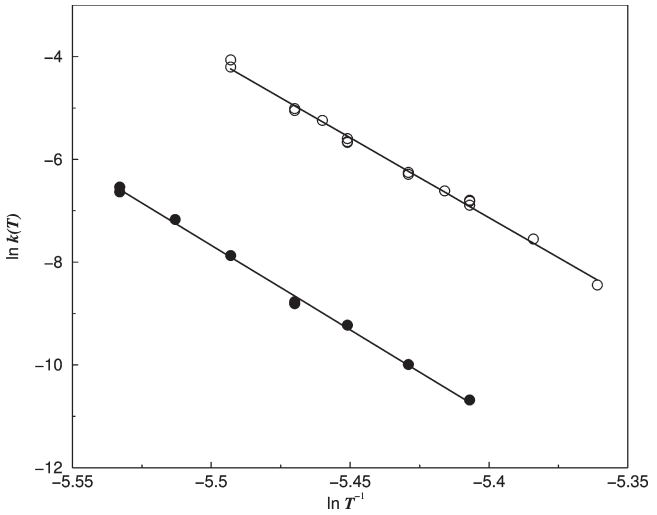

Figure 3. Arrhenius plot of H and D transfer rate constants of a bis (μ-oxo)dicopper complex with benzyl ligands, based on corrected data supplied by Tolman et al.[30b]

the values listed in Table 1, which show poor agreement between H and D data. The average transfer distances are 0.92 ± 0.07 and 0.80 ± 0.11 Å, respectively; including the WT data as well, the average value of r_0 for all three enzymes is 0.85 Å, the same as that in ref 29, which would indicate strong hydrogen bonding. In view of the large experimental error margins of the activation energies and especially the improbably low value for the H-transfer activation energy in the I553L mutant, it is not clear how much significance should be attached to the discrepancies.

The two remaining I553 mutants show substantially lower activity, indicating that the mutations, although relatively remote from the active site, are not completely innocent. For I553L we obtain $z(T) = 0.41 \pm 0.06$ and $\rho = 27 \pm 0.03$, corresponding to $r_0 = 0.93 \pm 0.04$ Å. Thus compared to the WT the transfer distance is larger, which reduces the effectivity of the tunneling mode and hence the activity of the enzyme but increases the contribution of the promoting mode, which compensates partly for the loss of activity. This behavior fits the expected pattern. However, that of mutant I553G does not. The vanishing activation energy for H transfer would imply that $z(T)F(T) \rightarrow 0$ and thus that $\hbar\omega_s \gg 4k_BT$ at room temperature, which is obviously not the case. On the other hand, the large activation energy observed for D transfer would imply $z(T) = 0.32$ and $\rho \simeq 28$, and thus $r_0 \simeq 0.96$ Å, i.e., again an increased transfer distance partly compensated by an increased contribution of the promoting mode so as to give rise to a reduced activity compared to the WT, a result consistent with that for the I553L mutant.

Comparing the series of I553 mutants with the WT enzyme, we note that in all of the mutants the transfer distance deduced from the D data is significantly larger than that from the H data. They all violate the condition that the activation energy for D transfer must not exceed twice the activation energy for H transfer, as given by eq 45. If this is indeed systematic, it might indicate that in the D isotopomer thermal excitation of the CD mode is starting to contribute, leading to E_a^D values larger than predicted by the model. A similar effect would be observed if overbarrier transfer would contribute to D transfer. However, that would not solve the main problem, which is the (near-)zero values for E_a^H observed in at least two of the mutants. Earlier we suggested that this may indicate interference of another slow step in the reaction sequence, but it seems unlikely that such a step would be temperature-independent. Since most of these discrepances disappear if error margins amounting to two standard deviations are accepted for the activation energies, it seems premature to attempt a more detailed analysis.

The final two mutants in Table 1 involve mutations closer to the active site and show strongly reduced activities but similar values for the KIE. The results of the analysis for the isotopes L546A and L754A are virtually indistinguishable: $z(T) = 0.46 \pm 0.03$ and $\rho = 31 \pm 1$, so that $r_0 = 1.01 \pm 0.03$ Å, i.e., a further increase of the transfer distance partly compensated by an increased contribution of the promoting mode relative to the I553 mutants. The promoting mode frequency will have adjusted accordingly, e.g., from 400 to 300 cm^{-1} for the same effective mass and even more if this mass is increased. However, these changes do not fully explain the observed absolute and relative activity of the two mutants. It may be that these mutations render the transfer endothermic; introduction of a term $\Delta E > 0$ is acceptable for mutant L456A and slightly improves the fit for mutant L754A. Moreover, mutations, as distinguished from isotope substitutions, affect not only the vibrational but also the electronic part of the transfer matrix element.

Compared to our earlier study[5] based on the golden rule, the instanton treatment offers a distinct improvement. It tightens up the results and removes some of the remaining problems. The analysis leads to a proton transfer distance of about 0.85 Å in agreement with the proposed nonadiabatic mechanism. It is remarkable that the mutations, even those that strongly reduce the activity, have barely an effect on the KIE. In this respect the

compensation of the effect of increasing transfer distances by that of increased promoting-mode contributions is virtually complete. Elsewhere[5] we have argued that this appears to be characteristic for transfer across hydrogen bonds.

6.5. CH Cleavage in a Bis(μ-oxo)dicopper Complex. An interesting model study is the investigation of hydrogen abstraction from an *N*-alkyl copper ligand of a bis(μ-oxo)dicopper complex by Tolman et al.,[30] who used it as a model for the active site of some monoxygenases. They measured rate constants for H and D transfer from an *N*-alkyl ligand to an oxygen bridging two coppers at temperatures between 213 and 253 K. Observing a large, temperature-dependent KIE, they concluded that the transfer proceeds by quantum-mechanical tunneling accompanied by transfer of an electron to a copper ion. The resulting Arrhenius plots[30b] displayed in Figure 3 give rise to the following kinetic parameters at $T = 233$ K: $\ln k^{H}(233) = -5.6$, $\ln \eta = 3.7 \pm 0.2$, $E_a^H/k_BT = 30.8 \pm 0.6$, and $E_a^D/k_BT = 33.5 \pm 0.5$. The large KIE combined with the low temperature of the measurements indicates that we can safely ignore overbarrier contributions to the transfer. Since the transfer is relatively slow and subject to a large activation energy, it appears to be endothermic and/or to involve a large reorganization term, which would not be surprising since it is not an enzymatic reaction. However, the calculated structure of the complex[31] indicates a transfer distance close to that estimated from van der Waals radii and standard bond lengths in the initial state. Since ΔE is obviously large, we cannot use eqs 40 and 41 but are restricted to eq 43, which does not depend on ΔE but does require an estimate of $F(T)$ and thus of ω_s. Taking $\omega_s \leq 200$ cm^{-1}, so that $F(T) \geq 0.94$ at 233 K, we obtain: $z(T) = 0.54 \pm 0.06$ and $\rho = 28 \pm 4$; substitution of these values in eqs 40 and 41 yields $\Delta E = (24.8 \pm 0.4)k_BT = 11.4 \pm 0.4$ kcal/mol; the lower limits correspond to the limit $F(T) = 1$. The values indicate nonadiabatic transfer in agreement with the mechanism originally proposed by Tolman et al.[30] and require the instanton method for a quantitative evaluation of the proton transfer distance. The values $r_0 = 0.95 \pm 0.03$ Å are comparable to but somewhat larger than that derived in section 6.4 for SLO1. Correspondingly, the promoting-mode frequency is lower: for $\omega_s \simeq 200$ cm^{-1} we obtain $\mu_s \simeq 17$.

6.6. Rice α-Oxygenase. Rice α-oxygenase (RαO) is a heme-containing dioxygenase, which attacks fatty acid C_α−H bonds, the first step being insertion of an oxygen molecule to form a hydroperoxide. Gupta et al.[32] reported recently that treatment of the enzyme with H_2O_2 enhances its activity and results in a persistent organic radical, an effect not shown by a mutant in which a tyrosine residue is replaced by phenylalanine. They also showed that the reaction exhibits a large KIE that is weakly temperature dependent. On the basis of these observations they propose that the initial C_α−H-cleavage step amounts to abstraction of a hydrogen atom by a tyrosyl radical, i.e., the same process as that found to be operative in galactose oxidase discussed in section 6.2.

However, the kinetic parameters tell a different story. While the GalOx reaction shows a relatively small KIE that is strongly temperature-dependent, the RαO reaction shows a large KIE that is weakly temperature-dependent, namely, $\ln \eta = 4.0$ and $\Delta E_a/k_BT = 1.9$ at 295 K at pH 10. Substitution in eq 43 yields $z(T) = 0.31$ with $\rho = 21$. These values are similar to those obtained in section 6.4 and clearly indicate an ionic transfer mechanism requiring an analysis in terms of the instanton rather than the golden rule approach. This leads to a transfer distance $r_0 = 0.82$ Å. For a promoting-mode frequency of 300 cm^{-1}, the effective mass amounts to about 17 hydrogen masses. Interestingly, at pH 7.2, both $\ln \eta$ and ΔE_a are reduced, the latter more than the former, which the authors ascribe to a competing reaction. The observed data, namely, $\ln \eta = 3.4$ and $\Delta E_a = 0.5$, are very similar to those for MADH[33] discussed in the next subsection, a reaction ascribed to ionic transfer, which equally suffers from kinetic complexity as follows from its failure to follow the Michaelis−Menten equation.

6.7. Methylamine Dehydrogenase and Related Enzymes. Scrutton and co-workers[33,34] have studied the oxidative demethylation of primary amines to form aldehydes and ammonia by methylamine dehydrogenase (MADH) and also by aromatic amine dehydrogenase (AADH), which shows much the same behavior. In these reactions a proton is abstracted by an active-site base from an iminoquinone intermediate, while an electron is transferred to a tryptophylquinone cofactor. Most of these reactions exhibit KIEs between 5 and 20 at 298 K with a very weak temperature dependence, although the rate constants show activation energies of more than 10 kcal/mol. The authors assumed that the proton-transfer step is rate determining. However, they report kinetics which do not follow the Michaelis−Menten equation; specifically the association and dissociation rate constants of the enzyme−substrate complex, denoted by k_1 and k_{-1} in eq 47, are subject to KIEs of the same general magnitude as k_{cat}. Our earlier efforts[3,4] to fit the data to a tunneling model were unsuccessful.

Our present analysis starts with the basic substrate methylamine,[33] for which a KIE of 16 ($\ln \eta = 2.8$) was measured. The observed effective activation energies $E_a^H/k_BT = 17.9$ and $E_a^D/k_BT = 18.5$, indicate that the reaction is endothermic. Application of eq 43, which is independent of ΔE, yields for $0.9 \leq F(T) \leq 1.0$ the values $z = 0.11 \pm 0.01$ and $\rho = 9.9 \pm 0.1$ which are incompatible with existing tunneling models; interpreted as due to nonadiabatic transfer, they yield a proton transfer distance of 0.58 Å, well outside the limit imposed by van der Waals radii and bond lengths. It indicates that these data are not representative of the properties of a single tunneling step. This is likely to be related to the observation that the kinetics does not follow eq 47. A similar complication was encountered in the preceding subsection; when the pH was increased, the KIE and its temperature dependence changed in a way that suggested the appearance of a competing reaction.[32]

Much the same holds for the data reported for a number of AADH reactions. However, the MADH reaction in which methylamine is replaced by ethanolamine[34] is an exception. The latter reaction exhibits the same KIE as the methylamine reaction, implying the same range of $z(T)$ values. While it has nearly the same activation energy for H transfer (17.6 against 17.9 in units of k_BT), its activation energy for D transfer is considerably larger (20.2 against 18.5 k_BT). As for methylamine, the reaction is clearly endothermic. We therefore first use eq 43 and afterward eqs 40 and 41. For for $0.9 \leq F(T) \leq 1.0$ we obtain $z = 0.83 \pm 0.11$, $\Delta E/k_BT = 9.5 \pm 1.5$, and $\rho = 30 \pm 3$. Interpreted as due to nonadiabatic proton transfer, these values lead to a transfer distance $r_0 = 1.00 \pm 0.05$ Å. For $\omega_s \simeq 200$ cm^{-1}, we have $\mu_s \simeq 14$. While these results look reasonable, some questions remain. In absolute terms, the rate of methanolamine conversion is much slower than that of methylamine conversion. Compared to the reaction catalyzed by SLO1 discussed in section 6.4, it is slower by a factor of about 30; however, if we correct for the effect of ΔE, it is faster by a factor of about 500 despite the larger transfer distance, while the KIE is much smaller and thus does

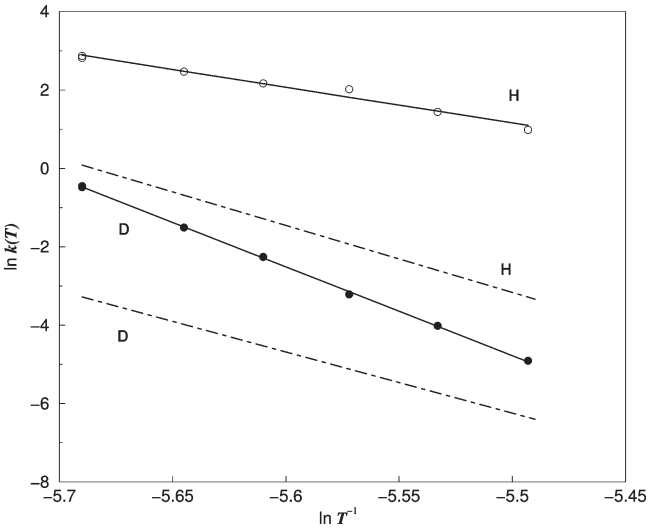

Figure 4. Arrhenius plot of H and D transfer rate constants of a benzylalcohol CH-oxidation reaction catalyzed by an oxoiron(IV) porphyrin radical cation. The circles, open for H and closed for D, and the solid lines represent the data reported in ref 35. The broken lines represent additional (unobservable) Arrhenius curves generated by the alternative transfer mechanism proposed in section 6.8; the top dot-dashed line depicts the H-transfer companion of the line drawn through solid circles and the bottom dot-dashed line the D-transfer companion to the line drawn through open circles.

not rule out the possibility of a substantial overbarrier contribution, especially to D transfer. Overall, the MADH and AADH data show several unusual features that remain to be explained.

6.8. CH Oxidation by an Oxoiron(Iv) Porphyrin Radical Cation. Our next example concerns oxidation of a CH bond by iron-containing enzymes, such as cytochrome P450. Specifically, we consider the very large deuterium isotope effects observed by Pan et al.[35] in the model study of CH-bond oxidation in benzylalcohol by an oxoiron(IV) porphyrin radical cation, namely, $(TMP)^{+\bullet}Fe^{IV}(O)(ClO_4^-)$. Pan et al. reported pseudo-first-order rate constants for benzylic CH and CD oxidation in acetonitrile at six temperatures in the range $T = 243-296$ K; their results and the corresponding Arrhenius plots are shown as circles and solid lines in Figure 4. The corresponding kinetic parameters at $T = 273$ K are $E_a^H = 5.0$ kcal/mol, $E_a^D = 12.0$ kcal/mol, $\ln \mathcal{A}^H = 11.3$, and $\ln \mathcal{A}^D = 19.8$. The authors commented on the unusual difference between the two activation energies and the two Arrhenius frequency factors. They pointed out that the Arrhenius parameters for CD oxidation behave almost classically, while those for CH oxidation indicate dominant tunneling, as does the large KIE (85 at 273 K, near the center of the temperature range, increasing to 360 at 243 K). To fit the data to the 1D Bell model, they had to assume different barriers for H and D transfer, which would signify a highly improbable breakdown of the Born–Oppenheimer approximation. Evidently, introduction of a non-zero value for ΔE would only worsen the problem.

According to eq 45, the maximum value of the ratio E_a^D/E_a^H, reached when $\Delta E = 0$ and $z(T) \ll 1$, equals Q^2, which is 1.85 in our estimate and will always be smaller than 2. Also, the maximum value of the difference between the two observed activation energies expressed in units k_BT, reached when $F(T) = 1$ and $z(T) \gg 1$, equals 2 ln η. Both conditions, applying at opposite ends of the $z(T)$ range, are strongly violated, the discrepancies being well outside the range of experimental error. It follows that the data are incompatible with a model in which both H and D transfer are governed by the same tunneling process. If H transfer is governed by tunneling, as the large KIE implies, then D transfer is either dominated by overbarrier transfer or by a different tunneling process. In either case, the observed rate constants $k^{H,D}(T)$ will be the sum of two components, $k_q^{H,D}(T)$ and $k_r^{H,D}(T)$, where the q-component, associated with H tunneling, will have a much smaller activation energy than the r-component associated with the alternative transfer process. In general, the corresponding Arrhenius plots should thus be curved. The observation that they are linear over a range of 50 K implies that in both cases one of the two components dominates, such that we can rewrite the expressions

$$k^H(T) = k_q^H(T)[1 + k_r^H(T)/k_q^H(T)],$$
$$k^D(T) = k_r^D(T)[1 + k_q^D(T)/k_r^D(T)] \quad (48)$$

in the form

$$\ln k^H(T) = \ln k_q^H(T) + k_r^H(T)/k_q^H(T),$$
$$\ln k^D(T) = \ln k_r^D(T) + k_q^D(T)/k_r^D(T) \quad (49)$$

where the linearity indicates that the second terms are not much larger than twice the error margins of the first terms. This allows us to roughly locate the Arrhenius curves of the hidden components $k_r^H(T)$ and $k_q^D(T)$ in Figure 4. The H-component of the r-process will be located between the two observed curves in a position such that at 296 K we have $0.62 \le k_r^H(T) \le 2.8$ in units s^{-1}, which implies a KIE in the range $1 \le \eta_r \le 4.5$ for the alternative process at this temperature. The hidden D component of the q-process will be located below the observed Arrhenius curves, so that we will only have an upper limit for $k_q^D(T)$, namely, 7×10^{-4} s^{-1} at 243 K, corresponding to $\ln \eta_q \ge 8.2$ at this temperature. The two hidden components are tentatively depicted by broken lines in Figure 4; the q-component is represented by a curve corresponding to the upper limit $\ln \eta_q = 8.2$ at 243 K and the r-component by a curve corresponding to $\ln \eta_r = 1$ at 296 K, on the basis of the following analysis.

Because we can carry out our standard analysis only at 243 K for H transfer via the q-component and at 296 K for D transfer via the r-component, the internal check provided by comparison of H and D results for the same transfer process is not available. Moreover, the KIE values for the q- and r-processes are only rough estimates. Therefore, we search for parameter values that roughly match those found in previous subsections, to determine whether a plausible interpretation of this type is possible. It turns out that a satisfactory description for the q-process can be obtained if we set $\ln \eta_q = 8.2$, as above, and $\Delta E = 6k_BT$, the result being $z(243) = 0.16$ and $\rho = 32$. These values are incompatible with adiabatic transfer. Assuming nonadiabatic transfer, we use the instanton approach, which yields a transfer distance of 0.98 Å comparable with the distances obtained in sections 6.4 and 6.5. Hence, this process is interpreted as nonadiabatic endothermic proton tunneling weakly supported by symmetric skeletal modes. The relatively large transfer distance and the small contribution of the promoting mode gives rise to the largest KIE hitherto observed in enzymatic (model) systems.

A totally different picture applies to the r-process that governs the Arrhenius curve observed for D-transfer. To obtain a satisfactory interpretation of this process in terms of the tunneling

Table 2. KIEs and Activation Energies of the Enzymatic Reactions Analyzed in Section [6] Together with the Model Parameters Derived from the Displayed Numbers and the Proton Transfer Distances (in Å) Deduced from These Parameters[a]

enzyme	$\ln \eta$	E_a^H/k_BT	E_a^D/k_BT	$\Delta E_a/k_BT$	$z(T)$	ρ	r_0	ref
MMCoAM	3.8	31.0	37.6	-	2.38	152	1.83	20
NeopentylCbl	3.4	-	-	5.3	2.4	153	1.8	22
GalOx	2.8	-	-	4.2	2.6	130	1.7	23
PheH	2.5	-	-	4.0	3.5	180	2.0	26
Lin/SLO1	4.4	2.8	5.3	-	0.26	21	0.83	27
Ara/SLO1	4.6	2.4	7.0	-	0.25	22	0.85	29
DiCu(Bn_3)	3.7	30.8	33.5	2.7	0.54	28	0.95	30
RαO/pH 10	4.0	-	-	1.9	0.31	21	0.82	32
RαO/pH 7.2	3.4	-	-	0.5	-	-	-	32
$MeNH_2$/MADH	2.8	17.9	18.5	0.6	-	-	-	33
$EtOHNH_2$/MADH	2.8	17.6	20.2	2.6	0.83	30	1.00	34
$Fe^{IV}O$(H)	(8.2)	9.3	-	-	(0.16)	(32)	(0.98)	35
$Fe^{IV}O$(D)	(1.0)	-	22.1	-	(5.6)	160	(1.8)	35

[a] Numbers in parentheses are tentative as explained in the text.

model, we have to assume that $\ln \eta_r \simeq 1$ and $\Delta E \simeq 0$; this yields $z(296) = 5.6$ and $\rho = 160$. The latter value indicates adiabatic transfer of a neutral hydrogen atom of the type discussed in sections 6.1 and 6.2, which can be treated by the golden rule; it leads to a transfer distance of 1.78 Å. The large value of $z(T)$ signals a dominant overbarrier contribution to the r-process and thus a corresponding Arrhenius curve for H transfer that is close to that for D transfer. The presence of two transfer processes, one labeled q dominating H- and the other labeled r dominating D-transfer can be plausibly traced back to the fact that the catalyst is a radical cation that can react both as an ion and as a free radical. Hence, it is possible to find a plausible interpretation for the very large KIE effects and anomalous activation energies reported by Pan et al. in terms of the present model.

A summary of the principal results derived in this section is listed in Table 2.

7. DISCUSSION

The kinetics of enzymatic reactions that exhibit large deuterium isotope effects are usually reported in Arrhenius form, i.e., as rate constants depending exponentially on temperature. The isotope dependence of the two parameters of this equation, the activation energy and the frequency factor, can tell us whether tunneling contributes to the reaction, but little else. To extract more useful information from such data for systems for which quantum-chemical input is not readily available, we have developed semiempirical methods in a recent series of articles,[3−5] which the present article extends to the instanton approach.

This approach, as formulated in the approximate instanton method (AIM) and implemented in the DOIT program,[18,19] has proved to be an efficient method to calculate tunneling splittings and tunneling rates from the structure and force field of only the three stationary structures along the reaction path. In this contribution, we show that the same approach remains useful for complex systems such as enzymes, for which such structures cannot be readily evaluated. For such systems, it will often be possible to reverse the procedure and to derive structural properties directly from an analysis of the temperature and isotope dependence of the observed rate constants. The key observation is that the KIE and its temperature dependence are related by a simple analytical relation formulated in terms of quantities that can be estimated empirically. Since for each isotope there is such an equation based on the same empirical parameters, there is often enough information to calculate specific physical properties of the system. These include the mechanism of the transfer, i.e., adiabatic or nonadiabatic, the transfer distance of the tunneling particle, the properties of the transverse modes promoting the tunneling, the endothermicity of the reaction, if any, and, last but not least, the compatibility of the kinetic data with a specific tunneling model.

While the formulation in section 4 in terms of the model parameters $z(T)$ and ρ should have general validity for approximately linear transfer paths, it should be realized that the relation of these parameters to observables, such as the transfer distance and the promoting-mode frequency, depends on the chosen form of the transfer potential via the coefficients $c_{1,2}$. Of the two chosen potentials, the one based on two crossing parabolas is clearly a limiting case. The other, based on the quartic potential, was earlier found effective for tunneling along a hydrogen bond. The present test indicates that it is also useful for the analysis of enzymatic CH-cleavage reactions. At the levels probed thus far it is proving superior to the golden rule approach, in that it applies both to adiabatic and nonadiabatic proton transfer. The extension of the applicability of the golden rule to nonadiabatic reactions requires estimates of the anharmonicity of the oscillators in the wells. This is very difficult if there is hydrogen bonding. It also requires generalization of the overlap integrals between the anharmonic oscillators to integrals over vibrational coordinates that couple the two wave functions. As a consequence, too many uncertain parameters enter into the formulas. The instanton approach is based on a quartic potential that has proved its usefulness in earlier calculations on small systems. Moreover, we demonstrated that it leads to a formula of the same general form as that for crossing harmonic potentials, leaving room for generalization to intermediate potentials whenever these become available.

For the moment, the main advantage of the generality of this form is that the kinetic data can be analyzed irrespective of whether the transfer mechanism is known. The model predicts and the examples confirm that the two model parameters ρ and $z(T)$ assume very different values for adiabatic and nonadiabatic transfer, thus allowing easy identification. Once the mechanism is established, physical parameters such as the transfer distances

and the properties of the promoting mode can be calculated and compared with available experiments or calculations, from which conclusions can be drawn about the plausibility of the results.

To demonstrate the use and explore the usefulness of this approach, we have analyzed eight groups of enzymatic CH-cleavage reactions for which appropriate kinetic data are available. The data required are rate constants together with their temperature and isotope dependence in a temperature interval near or below room temperature. An analysis may still be possible if the data are obtained by product analysis, where the measured activation energy is limited to the KIE, but the results will be more limited. Since the equations apply only to throughbarrier transfer, the KIE should be large enough to indicate a reaction dominated by tunneling. In principle, the method can be extended to mutants, but it should be borne in mind that there may be an electronic contribution to the difference in rates between systems differing by a mutation.

As Table 2 demonstrates, the analysis separates the CH-cleavage reactions studied into two distinct groups. In the first, comprising the top three reactions, the temperature dependence of the KIE, expressed as an activation energy in units of the thermal energy, exceeds the natural logarithm of the KIE. For these systems, the transfer distance amounts to about 1.8 Å, as expected for transitions between two carbon centers. The relatively large contribution of skeletal modes to the transfer coordinate points toward multiple low-frequency promoting modes that are thermally excited at room temperature. The mechanism in which a free carbon-centered radical abstracts a neutral hydrogen atom from a CH bond was confirmed in two of the eight systems, the B_{12}-type enzyme discussed in section 6.1 and galactose oxidase discussed in section 6.2. It is likely that there is a third member of this group, namely, phenylalanine hydroxylase, discussed in section 6.3, in view of the strong temperature dependence of the relatively small KIE, but this small KIE suggests contributions from overbarrier processes that may be large enough to cast doubt on the analysis.

The remaining five systems all show clear evidence of a totally different transfer mechanism, in which the temperature dependence of the KIE, expressed as above, is much smaller than the logarithm of the KIE. The derived transfer distance of about 1 Å or less points toward a path shortened by hydrogen bonding, which identifies the tunneling particle as a proton and the acceptor atom as oxygen. Correspondingly, the promoting mode along the hydrogen bond has a relatively high frequency ($200-400\ cm^{-1}$) and will be only weakly excited at room temperature. Since the neutral CH bond is nonpolar, the hydrogen bonding implies electron withdrawal from this bond by a redox center. This ionic mechanism is confirmed for three of the five systems and proposed for the other two, i.e., those discussed in sections 6.6 and 6.8, where the mechanism was not yet convincingly established.

Of the confirmed mechanisms, the data on the lipoxygenase-1 reaction, discussed in section 6.4, are by far the most complete since they are accompanied by data for several mutants. The derived parameters indicate an ionic reaction, in agreement with other evidence. Compared to the free radical mechanism, it shows a larger KIE with, however, a considerably weaker temperature dependence, the latter property being due to the higher frequency of the promoting mode, which in turn results from the presence of hydrogen bonding along the ionic transfer path. The analysis leads to a proton transfer distance of about 0.85 Å along with an effective mass and frequency of the promoting that is typical for hydrogen bonding. The implied strong hydrogen bonding may indicate that in this reaction electron transfer precedes proton transfer.

The mutants generally support this picture, but some tend to show activation energies for H transfer that are too low compared to those for D transfer and also too low, in an absolute sense, to be compatible with accepted tunneling models. However, the error margins of the Arrhenius plots are very wide, leaving room for considerable experimental uncertainty. A typical effect of mutation is an increase in the transfer distance partly compensated by an increase in the promoting-mode contribution.

The analysis was successfully applied in section 6.5 to a model enzymatic reaction in which an oxygen bridging two coppers abstracts a proton from an *N*-alkyl ligand. The derived parameters fit the presumed ionic mechanism; they are in the same ballpark as those found for lipoxygenase-1, showing a somewhat larger transfer distance, namely, about 1.0 Å, and correspondingly weaker hydrogen bonding as indicated by a lower promoting-mode frequency, in agreement with the observations discussed in the preceding paragraph.

Our interpretation of the kinetic data of the remaining three systems differs from that proposed by the authors. While the parameters derived in section 6.6 for rice α-oxygenase indicate unambiguously that the transfer mechanism is ionic, the authors of the data tentatively opted for a free radical interpretation. Our opposite point of view is supported by a comparison with kinetic data for CH-bond cleavage in galactose oxidase. The deviations in the remaining two systems we ascribe to kinetic complexity, i.e., the presence of competing reactions. In the case of methylamine dehydrogenase discussed in section 6.7, the failure of the rate constants to follow the Michaelis−Menten mechanism shows evidence for such complexity. Our interpretation is further supported by a comparison with the kinetic data for Rice α-oxygenase at a pH of 7.2, where a similar complexity appears. The kinetic complexity in the case of the oxoiron(IV) porphyrin radical cation $(TMP)^{+\bullet}Fe^{IV}(O)(ClO_4^-)$ discussed in section 6.8 follows from the observation that the kinetic data for H and D transfer cannot be accounted for on the basis of accepted tunneling models. The data can be explained, however, if we assume two competing mechanisms of which the one dominated by tunneling governs H transfer and the other dominated by an overbarrier process governs D transfer.

8. CONCLUSION

This paper shows that the analysis of kinetic isotope effects in enzymatic CH-cleavage reactions can easily be carried beyond the standard Arrhenius equation. To this end we present a number of semiempirical equations derived from instanton theory for application to kinetic data for reactions presumed to be dominated by tunneling. The equations are easy to apply to rate constants for H and D transfer measured as a function of temperature. This leads to values for two model parameters, ρ and $z(T)$, which can be used to derive two physical parameters, the equilibrium transfer distance r_0 of the tunneling particle and the mass μ_s and frequency ω_s of the (effective) promoting mode if the mechanism of the reaction, namely, adiabatic transfer of a neutral H radical or nonadiabatic transfer of a proton accompanied by electron transfer, is known. The theoretical model claims and the examples treated confirm that the numerical values of the model parameters will be very different for the two mechanisms, which should make it easy to derive the physical parameters if the model is applicable.

In principle, the application can thus lead to any of three results: (i) The transfer is adiabatic with ρ in the neighborhood of 150 and $z(T) > 1$ near room temperature. In that case, we can use the harmonic form of the equations, obtained either by instanton theory or the golden rule, to derive a value for r_0. The promoting mode is an effective mode made up of several low-frequency modes, and its mass and frequency remain undetermined; the large $z(T)$ value is due to thermal excitation of the low-frequency modes. (ii) The transfer is nonadiabatic with ρ in the range 20−40 and $z(T) < 1$ near room temperature. In that case, we should use the quartic form of the equations obtained by instanton theory, which is superior to anharmonic forms obtained from the golden rule, to derive values for r_0 and for the combination μ_s, ω_s; the latter values should reflect the properties of a $C^{(+)}$−H···O-stretching mode. (iii) The application fails to generate acceptable parameter values. There are many possible causes for failure, including inadequacy of the model, but based on the examples treated above, we suggest that the most probable cause is kinetic complexity, i.e., competition of other rate processes. If the KIE is 10 or less, competition of overbarrier transfer should be expected. Failure of the data to obey the limiting rules described in section 4 is an indication that the data do not represent a single tunneling step in the reaction sequence.

On the basis of the data presently available, we propose that the model can reliably determine the mechanism of the transfer and is a good indicator of unforeseen kinetic complications. The accuracy of the predicted physical parameters, in particular, the tunneling distance, can only be established by measurements or calculations at a higher level. For the time being, their main use may be qualitative, e.g., by allowing comparison of closely related reactions.

AUTHOR INFORMATION

Corresponding Author

*E-mail: willem.siebrand@nrc-cnrc.gc.ca.

ACKNOWLEDGMENT

We thank Professor William Tolman for his permission to report here the unpublished corrected data depicted in Figure 3.

REFERENCES

(1) Benderskii, V. A.; Makarov, D. E.; Wight, C. H. *Adv. Chem. Phys.* **1994**, *88*, 1.
(2) Truhlar, D. G. *J. Phys. Org. Chem.* **2010**, *23*, 660.
(3) Siebrand, W.; Smedarchina, Z. *J. Phys. Chem. B* **2004**, *108*, 4185.
(4) Siebrand, W.; Smedarchina, Z. In *Isotope Effects in Chemistry and Biology*; Kohen, A., Limbach, H.-H., Eds.; Taylor & Francis: Boca Raton, FL, 2006; pp 725−741.
(5) Siebrand, W.; Smedarchina, Z. *J. Phys. Org. Chem.* **2010**, *23*, 620.
(6) Siebrand, W.; Wildman, T. A.; Zgierski, M. Z. *J. Am. Chem. Soc.* **1984**, *106* (4083), 4089.
(7) Smedarchina, Z; Siebrand, W.; Zgierski, M. Z.; Zerbetto, F. *J. Chem. Phys.* **1995**, *102*, 7024.
(8) Smedarchina, Z; Siebrand, W.; Zgierski, M. Z. *J. Chem. Phys.* **1995**, *103*, 5326.
(9) Smedarchina, Z; Siebrand, W.; Zgierski, M. Z. *J. Chem. Phys.* **1996**, *104*, 1203.
(10) Fernández-Ramos, A.; Smedarchina, Z; Zgierski, M. Z.; Siebrand, W. *J. Chem. Phys.* **2004**, *109*, 1004.
(11) Smedarchina, Z.; Fernández-Ramos, A.; Siebrand, W. *J. Chem. Phys.* **2005**, *122*, 134309.
(12) Smedarchina, Z.; Fernández-Ramos, A.; Siebrand, W. *Chem. Phys. Lett.* **2004**, *395*, 339.
(13) Siebrand, W.; Smedarchina, Z. *Int. Rev. Phys. Chem.* **1999**, *18*, 5.
(14) Marcus, R. A. *J. Chem. Phys.* **1956**, *24*, 966.
(15) Benderskii, V. A.; Goldanskii, V. I.; Makarov, D. E. *Chem. Phys.* **1991**, *154*, 407.
(16) Smedarchina, Z.; Siebrand, W.; Fernández-Ramos, A.; Martínez-Núñez, E. *Chem. Phys. Lett.* **2004**, *386*, 396.
(17) Smedarchina, Z.; Siebrand, W. *Chem. Phys. Lett.* **2005**, *410*, 370.
(18) Smedarchina, Z.; Fernández-Ramos, A.; Siebrand, W. *J. Comput. Chem.* **2001**, *22*, 787.
(19) Smedarchina, Z.; Fernández-Ramos, A.; Zgierski, M. Z.; Siebrand, W. *DOIT 2.0, a computer program to calculate hydrogen tunneling rate constants and splittings*; 2004.
(20) Chowdhury, S.; Banerjee, R. *J. Am. Chem. Soc.* **2000**, *122*, 5417.
(21) Doba, T.; Ingold, K. U.; Reddoch, A. H.; Siebrand, W.; Wildman, T. A. *J. Chem. Phys.* **1984**, *8*, 6622.
(22) Doll, K. M.; Finke, R. G. *Inorg. Chem.* **2003**, *42*, 4849.
(23) Whittaker, M. M.; A.; Ballou, D. P.; Whittaker, J. W. *Biochemistry* **1998**, *37*, 8426.
(24) Fitzpatrick, P. F. *Biochemistry* **2003**, *42*, 14083.
(25) Bassan, A; Blomberg, M. R. A.; Siegbahn, P. E. M. *Chem.—Eur. J.* **2003**, *9*, 4055.
(26) Pavon, J. A.; Fitzpatrick, P. F. *J. Am. Chem. Soc.* **2005**, *127*, 16414.
(27) Knapp, M. J.; Rickert, K. W.; Klinman, J. P. *J. Am. Chem. Soc.* **2002**, *124*, 3865.
(28) Meyer, M. P.; Tomchick, D. R.; Klinman, J. P. *Proc. Natl. Acad. Sci. U.S.A.* **2008**, *105*, 1146.
(29) Jacquot, C.; Peng, S.; van der Donk, W. A. *Bioorg. Med. Chem. Lett.* **2008**, *18*, 5959.
(30) (a) Mahapatra, S.; Halfen, J. A.; Tolman, W. B. *J. Am. Chem. Soc.* **1996**, *118*, 11575.(b) Tolman, W. B. Corrected data (private communication). Only the complex with benzyl ligands is used in our analysis since a peroxo isomer may contribute to the complex with isopropyl ligands.
(31) Cramer, C. J.; Pak, Y. *Theor. Chem. Acc.* **2001**, *105*, 477.
(32) Gupta, A.; Mukherjee, A.; Matsui, K.; Roth, J. P. *J. Am. Chem. Soc.* **2008**, *132*, 11275.
(33) Basran, J. B.; Sutcliffe, M. J.; Scrutton, N. S. *Biochemistry* **1999**, *38*, 3218.
(34) Basran, J. B.; Patel, S.; Sutcliffe, M. J.; Scrutton, N. S. *J. Biol. Chem.* **2001**, *276*, 6234.
(35) Pan, Z.; Horner, J. H.; Newcomb, M. *J. Am. Chem. Soc.* **2008**, *130*, 7776.